

1 **Constraints on syn-rift intrabasinal horst development from alluvial-fan and aeolian deposits**
2 **(Triassic, Fundy Basin, Nova Scotia).**

3
4 Sophie Leleu^{1,2,*} and Adrian J. Hartley¹,

5
6 ¹*School of Geosciences, University of Aberdeen, Aberdeen, AB24 3UE, Scotland, UK*

7 ²*Present day address: Bordeaux-INP, ENSEGID, EA4592 G&E, Université Bordeaux Montaigne , 1 allée*
8 *Daguin, 33607 Pessac, France*

9 * *Corresponding author: sophie.leleu@ensegid.fr*

10
11 **Number of words, Number of references, Number of tables and figures**

12
13 **Running title:** Intrabasinal alluvial fans during horst development

14
15 **ABSTRACT (< 200 WORDS)**

16 The Triassic Fundy rift basin was a large (>70 km wide) half-graben filled with alluvial, lacustrine and aeolian
17 deposits. A major lithospheric lineament, the Cobequid-Chedabucto Fault Zone (CCFZ) which forms the tip
18 of the Newfoundland-Gibraltar Fault Zone, occurs within the Fundy Basin. The timing of early movement on
19 this important fault zone is poorly constrained. Here we present data from the alluvial and aeolian units that
20 crop out adjacent to the CCFZ in the Minas sub-basin to determine the initiation of fault movement. We use
21 the onset of alluvial-fan deposition to infer when the fault became sufficiently active to create intrabasinal
22 topography and document the influence of fault activity on intrabasinal drainage. The occurrence and
23 preservation of aeolian deposits immediately adjacent to the CCFZ and concomitant with alluvial-fan
24 development suggests a wind-shadow effect associated with fault-generated topography. The onset of alluvial-
25 fan deposition associated directly with the fault occurred during Norian times, following an earlier phase of
26 sedimentation in the Fundy Basin, and records a potentially important phase of plate reorganisation during
27 early Atlantic rifting.

28

29 Triassic basin-fill successions present along the North American Seaboard have been the focus for studies of
30 continental stratigraphy (e.g Cornet, 1977; Olsen et al., 1982; Olsen and Sues, 1986; Olsen et al., 1989;
31 Fowell and Traverse, 1995; Whiteside et al., 2007; Lucas and Tanner, 2007; Cirilli et al., 2009), sedimentary
32 evolution of rift basins (Smoot, 1991; Schlische and Olsen, 1990; Olsen, 1997; Leleu & Hartley 2010) and
33 structural development of rift basins (e.g. Olsen and Schlische, 1990; Schlische, 1993; Withjack et al., 1995,
34 1998; Olsen, 1997). One of the key studied basins is the Fundy Basin due to excellent exposure and a
35 subsurface database (Olsen and Schlische, 1990; Schlische, 1993; Wade et al., 1996; Withjack et al., 1995,
36 1998). Recent studies have considered sediment distribution at a basin scale in the Fundy Basin in relation to
37 the tectonic framework (Leleu & Hartley, 2010; Leleu et al., 2009, 2010). Most previous studies have
38 considered the present-day geomorphology of the Fundy Basin to be largely inherited from Triassic times as
39 palaeogeographic models for the Late Triassic are basically based on present-day relief (e.g. Hubert & Mertz,
40 1984; Hubert & Forlenza, 1988). Late Triassic palaeogeographical representations consider the major fault
41 zone in the centre of the Fundy Basin, the Cobequid-Chedabucto Fault Zone (CCFZ), to be a permanent
42 feature during sedimentation with fluvial drainage networks derived from the uplifted fault block and draining
43 southwards into the basin (Hubert & Mertz, 1984; Hubert & Forlenza, 1988). To assess the validity of these
44 models and to constrain the timing of movement on this important fault system we examine the sedimentary
45 succession exposed immediately adjacent to it. Thus recognition of alluvial-fan deposits and their integration
46 within a stratigraphic context is crucial to evaluate the history of fault activity. The CCFZ links with the
47 Newfoundland-Gibraltar Fault Zone and the timing of movement could yield important information regarding
48 the onset of Atlantic rifting. At a more local scale, understanding drainage development within the basin
49 allows the reconstruction of uplift history of the horst structure and how it modified drainage and sediment
50 distribution. This paper highlights the problem of identifying structural and sedimentary linkages between
51 different sub-basins in rift systems and aims to constrain the timing of fault movement using the development
52 of alluvial-fan sedimentation adjacent to the CCFZ.

53

54 **GEOLOGICAL SETTING**

55 The Fundy Basin forms one of a series of NE-trending early Mesozoic rift basins developed along the Atlantic
56 North-American margin following the trend of Caledonian structures (e.g. Manspeizer, 1988). It contains 6 to
57 12 km of Anisian to basal Hettangian non-marine clastic sediments in its depocenter (Olsen et al., 1989;
58 Fowell and Traverse, 1995; Wade et al., 1996; **Figs. 1, 2**). The present-day basin is approximately 200 km in
59 length and 70 km in width, and is divided into three structurally distinct sub-basins: the Minas, Chignecto and
60 Fundy sub-basins, assumed to form a complex half-graben system (Wade et al., 1996; **Fig. 1A, B, C**). The
61 Minas sub-basin is one of the rare E-W trending basins present along the North American margin and its
62 orientation is probably related to the structural control imparted by the Caledonian Cobequid-Chedabucto
63 Fault Zone (Schlische, 1993). This fault zone was reactivated with a strike-slip component during the latest
64 Triassic and earliest Jurassic (Olsen and Schlische, 1990; Withjack et al., 1995). The Triassic succession in
65 the Minas sub-basin forms a broad syncline that was subsequently inverted (**Fig. 1D**; Withjack et al, 1995)
66 due to movement on the CCFZ which resulted in faulting and fragmentation of the northern edge of the Minas
67 sub-basin such that the overall Triassic depositional geometry on the northern basin margin is difficult to
68 constrain (Withjack et al. 2009). The CCFZ itself is a complex fault zone with 2 major faults trending E-W
69 and many smaller scale faults, some of which trend NE-SW (Olsen & Schlische 1990; **Fig. 1A, 3**).

70

71 **Structural background**

72 Published cross-sections based on seismic surveys are available and provide a structural framework for the
73 basin (e.g. Schlische, 1993; Wade et al., 1996; Withjack et al., 2010). The Fundy Basin border fault
74 corresponds to a re-activated low-angle Caledonian thrust fault that trends NE-SW (Schlische, 1993; Withjack
75 et al., 1995). The border faults are the Chignecto Fault in the Chignecto sub-basin and the Headlands Fault
76 running along the New Brunswick coastline in the Fundy sub-basin. The interpreted seismic profile (**Fig. 1A,**
77 **B, C**) shows the development of a sedimentary wedge thickening towards the border faults.

78

79 The present-day Minas sub-basin is defined to the south by the contact of Triassic sediments and the southern
80 granitic uplands, and to the north by the CCFZ. There are limited structural data for the Minas sub-basin with
81 only one recent study illustrating one N-S section (**Fig. 1D**) and one NE-SW section in the western part

82 (Fig.1B; Withjack et al., 2010), but the relationships between stratigraphic units and faults are not obvious on
83 these sections. A seismic profile through the western part of the Minas sub-basin and one through the Fundy
84 sub-basin (Fig. 1B, C) show that Triassic sediments thicken towards the CCFZ, suggesting that the fault was
85 active during deposition. Detailed field studies along the northern Minas coast show that strike-slip motion
86 occurred along the CCFZ during earliest Jurassic times (Olsen & Schlische, 1990; Withjack et al., 2009;
87 2010). Olsen & Schlische (1990) recorded complex fault patterns interpreted as part of a larger scale left-
88 oblique slip along the fault system during early Mesozoic extension (Fig. 3). Despite the complex outcrop
89 pattern, the sedimentary succession close to the CCFZ can be reconstructed and applied to constrain the
90 development of the northern margin of the Minas sub-basin during the Late Triassic. The studied sections are
91 highly faulted and located three to five kilometres south of the main inland fault.

92

93 **Stratigraphy of the Fundy Basin**

94 Two main sedimentary packages fill the Fundy Basin and are recognized in seismic lines. The lower coarser
95 unit is referred to as the Wolfville Formation and the upper finer unit is the Blomidon Formation (Fig. 2). The
96 North Mountain Basalt conformably overlies the Blomidon Formation and is part of the Central Atlantic
97 Magmatic Province (CAMP). These units are best exposed in the Minas sub-basin where they are dated as
98 Late Triassic (Carnian to Rhaetian). The main volcanic phase of CAMP development is Rhaetian in age (e.g.
99 Cirilli et al., 2009). The succession in the Chignecto sub-basin is not easily related to the units imaged
100 offshore, most of which are considered older in age and likely represent the lowermost Triassic deposits
101 present in the basin (Olsen et al., 2000; Leleu & Hartley, 2010). The Chignecto sub-basin comprises a 1600 m
102 thick Triassic fluvial succession (the Quaco Formation and the overlying Echo Cove Formation) that rests
103 unconformably on Permian strata (Nadon and Middleton, 1985; Olsen et al., 2000). The Quaco Formation
104 consists of conglomerates interpreted to be the product of a large fluvial system flowing northwards (Klein,
105 1962; Nadon and Middleton, 1985). The Echo Cove Formation includes slope deposits and fluvial sediments
106 that show palaeoflows towards the east-southeast and suggesting that sedimentation occurred on a fan (Nadon
107 and Middleton, 1985). The oldest sediments were considered to be middle to late Carnian but could be
108 Ladinian in age (Nadon and Middleton, 1985).

109

110 **Stratigraphy of the Minas sub-basin**

111 The Wolfville Formation lies unconformably on significantly older rocks and forms the main syn-rift unit in
112 the Minas sub-basin (Wade et al., 1996). The Wolfville Formation is Carnian in age but an older, Anisian age,
113 is hypothesised for one faulted outcrop along the northern shore (Olsen & Sues, 1986), known as the Carrs
114 Brook section (**Fig. 3A**) and along the CCFZ. These deposits are older than the Wolfville Fm and represent a
115 previous phase of rift development (Leleu & Hartley, 2010). Parts of the Echo Cove Formation in the
116 Chignecto sub-basin are probably contemporaneous with some of the Carnian Wolfville Formation.

117

118 Based on facies and sedimentary architecture, the Wolfville Formation has been sub-divided into 3 informal
119 units (**Fig. 4A-C**): the deposits of the lower and middle Wolfville Formation are interpreted as lateral
120 distributive fluvial input to the basin, flowing to the north and sourced from the southern rift shoulder (Leleu
121 et al., 2009, 2010; Leleu & Hartley, 2010). The lower Wolfville Formation corresponds to conglomeratic
122 sediments deposited by alluvial fans and highly mobile fluvial channels (Leleu et al., 2009). The middle
123 Wolfville Formation comprises sandy channel complexes and overbank deposits that represent the
124 downstream facies equivalent of the underlying conglomeratic system (Leleu et al., 2010). The upper
125 Wolfville Formation is interpreted as deposits of distal and smaller distributive fluvial systems, comprising
126 splays and subordinate channel deposits alternating with aeolian and ephemeral-lacustrine sediments (Leleu &
127 Hartley, 2010). These were deposited around 24/25° N (respectively Kent and Tauxe, 2005 and Van Houten,
128 1977) under semi-arid to sub-humid conditions (Tanner, 1993).

129

130 The Blomidon Formation overlies the Wolfville Formation (Olsen et al., 1989) and records a significant
131 change in facies architecture comprising mainly laminated lacustrine mudstones, massive playa mudstones
132 with occasional evaporites and patches of rippled sand within claystones, known as sandpatch fabrics (Hubert
133 and Hyde, 1982; Mertz and Hubert, 1990; Smoot, 1990; Ackermann et al., 1995; Tanner, 2000; Leleu &
134 Hartley, 2010; **Fig. 4D**). In the southern part of the basin it comprises sandy sheetflood deposits while finer-
135 grained lacustrine sediments dominate in the northern area in proximity of the CCFZ (Gould, 2001).

136

137 **SEDIMENTOLOGY OF THE LOWER ECONOMY DEPOSITS**

138 The sediments of the Minas sub-basin studied along the CCFZ are located in three main sections around the
139 locality of Lower Economy (**Fig. 3B**): the Economy Point Section, the Soley Cove Section and its lateral
140 “equivalent” ending at the Red Head Section of Five Islands, studied previously by Hubert & Mertz (1980,
141 1984). This contribution describes the first two sections in detail and their relationship to the Red Head
142 section. In the studied sections 11 lithofacies are recognised and described in **Table 1**, grouped into 4 facies
143 associations based on lithofacies and sedimentary architecture.

144 The **Alluvial-Fan** facies association comprises mainly clast-supported breccia (*lithofacies 1*), matrix-
145 supported breccia (*lithofacies 2*) and pebbly sandstones (*lithofacies 3*) (**Figs. 5A-E**). Breccias (*lithofacies 1*
146 *and 2*) record debris-flow and hyperconcentrated-flow deposition on alluvial fans while pebbly sandstones
147 (*lithofacies 3*) indicate more fluidal streamflow events (**Table 1**). The granule-bearing sandstones and isolated
148 sandsheet lithofacies (*lithofacies 4 and 6*) represent more distal fan-toe sediments (**Figs. 5F, G, H**) and are
149 intercalated with playa-margin facies (**Fig. 6**). The isolated sandsheet (*lithofacies 6*) may have been deposited
150 during the waning phase of flows which deposited the granule-bearing sandstone on the distal fan. The
151 angular nature of the clasts, the occurrence of oversized clast sizes (up to 1m), the locally derived lithologies of
152 the clasts (mainly gneiss and Carboniferous metasediments forming the present-day Cobequid High) and
153 interpreted sedimentary processes suggest that deposition on the alluvial fans was very close to the sediment
154 source and probably less than 8 to 10 km in length (e.g. Blair and McPherson, 1994).

155 The **Playa-Margin** facies association comprises mainly ripple-laminated sandstones (*lithofacies 8*), sand-
156 patch sandstones (*lithofacies 5*) and claystones (*lithofacies 11*) (**Figs. 5I-M**), intercalated with granule-bearing
157 sandstone (*lithofacies 4*) and locally with isolated sandsheets (*lithofacies 6*). The ripple-laminated sandstones
158 (*lithofacies 8*) represent distal sheetflood deposits (**Fig. 5K**), downstream equivalents to coarser
159 hyperconcentrated flows that left coarse sediments upstream on the fan surface (**Table 1**). They are
160 intercalated with granule-bearing sandstones (*lithofacies 4*) that correspond to coarser sheetflood deposits that
161 flowed further downstream on the fan surface. The ripple-laminated sandstones are typical deposits of the fan

162 toe and are intercalated with the playa claystones (**Fig. 6**). Claystones (millimetric to centimetric horizons)
163 drape ripples on top of the sheetflood deposits (*lithofacies 8*; **Fig. 5L**), and were likely deposited during
164 waning flow phase, whilst thicker units most likely accumulated in ephemeral ponds. Some interference
165 ripples (**Fig. 5M**) attest to the shallowness of the lake as wind-generated ripples reworked previous current
166 ripples. Sand-patch fabric sandstones (*lithofacies 5*; **Table 1**; **Figs. 5I, J**) also suggest low lake levels and
167 some periodic exposure, with the wind blowing across the wet playa surface generating “adhesion ripples”.
168 Soft sediment deformation of the ripples (**Fig. 5I**) is considered to be due to either evaporite dissolution
169 initially present on or just below the playa surface, or to bioturbation (**Table 1**). The association of sand-patch
170 sandstones (*lithofacies 5*) with ripple-laminated sandstones (*lithofacies 8*) and claystones (*lithofacies 11*) is
171 typical of the Blomidon Formation assigned to middle to late Norian and Rhaetian (Fowell and Traverse,
172 1995).

173 The **Fluvial** facies association comprises cross-stratified sandstones (*lithofacies 7*), siltstones (*lithofacies 9*)
174 and heterolithic deposits (*lithofacies 10*). It forms the Economy Point section that is over 30 metres thick of
175 which only the basal 23 metres are accessible for detailed description (**Fig. 7**). The association represents a
176 highly mobile fluvial system composed of large, amalgamated, multi-storey channel belts intercalated with
177 relatively thick units of overbank deposits (over 12 metres in thickness for some intervals). The fluvial
178 channel belts are wider than the outcrop length (> 4 km) and represent the amalgamation of migrating or
179 avulsing channels. Intervals of floodplain deposits are not very well exposed but comprise thin intercalated
180 claystones and sandstone beds that often show ripple cross-lamination (heterolithic deposits, *lithofacies 10*).
181 These deposits form either foresets composed of intercalated claystones and sandstones that prograde over
182 few meters and are interpreted as crevasse-splay deposits (**Table 1, Fig. 5N**) or comprise lenses of sandstones
183 overlying small-scale shallow erosional features in fine-grained floodplain deposits, interpreted as crevasse-
184 channel deposits.

185 The **Aeolian** facies association comprises quartzitic sandstones that were described in detail by Hubert &
186 Mertz (1980, 1984). They consist of rounded to subrounded quartz grains that are moderately to very well
187 sorted. The sandstones show preserved sets of large foresets up to 3.50 metres thick. Beds show either sub-
188 horizontal stratification or steep cross-beds. The latter comprise grainflow deposits that are preserved on dune

189 foresets and finer-grained well sorted grainfall deposits (Hubert & Mertz, 1980). Some cross-beds are
190 tangential and show pin-striped laminae representing aggradation during wind-ripple migration. Similar wind
191 ripples are present in the planar low-angle units and represent dune-toe deposits (Hubert & Mertz, 1984).
192 Large-scale erosion surfaces were recognised for over 300 meters laterally and truncate smaller scale aeolian
193 structures; they are horizontal with a few centimeters of erosional relief (Hubert & Mertz, 1980), and are
194 interpreted as first-order bounding surfaces representing dry interdune development between events of dune
195 accumulation (e.g. Brookfield 1977). Similar surfaces are often overlain by ventifact pebbles generally 2 to 4
196 cm in length, but locally pebble lags with pebbles up to 10 cm may be developed. Locally the quartzitic
197 sandstones (Aeolian facies association) are interbedded with beds of pebbly sheetflood deposits (**Figs. 50, 8**).
198 The latter correspond to the breccia and pebbly sandstones (Alluvial Fan facies association) described above
199 (see **Table 1**). These surfaces with pebble lags and occasionally overlain by alluvial deposits represent a
200 significant hiatus in the aeolian record during which waterlain processes eroded part of the aeolian dune field
201 and may represent super-surfaces (*sensu* Kocurek 1988). The aeolian deposits measured in the section at Red
202 Head of Five Island represent the thickest aeolian section and most abundant Triassic aeolian dune deposits of
203 the Minas sub-basin. Hubert and Mertz (1984) measured palaeoflow directions on aeolian dune foresets (n =
204 73) from the Red Head section with a mean palaeowind direction towards N254°.

205

206 **SEDIMENTARY ARCHITECTURE ALONG THE COBEQUID FAULT**

207 **Economy Point section**

208 At Economy Point (**Fig. 3**), laterally extensive outcrops (over 3 kilometres) of fine-grained fluvial deposits
209 show channel-fill deposits (units up to 13 metres) intercalated with floodplain deposits (3 to 12 metres). The
210 channel fills form large composite channel belt complexes passing laterally into splays and shaly floodplain
211 deposits. The splay deposits show dipping accretion of intercalated sandstone and claystone over tens of
212 meters. Palaeocurrent measurements from 3D fluvial cross-beds exposed on the present-day wavecut platform
213 (41 bedforms) show a relatively narrow range (azimuth between N005 and N110) with a mean palaeoflow to
214 the NE (azimuth N068). At Economy Point, the fluvial deposits are interpreted as middle Wolfville Fm. They
215 display identical lithofacies, similar sedimentary architecture and comparable palaeoflow direction (between

216 N019 and N050) to middle Wolfville deposits located 8 to 10 kilometres away along the southern shore at
217 Burntcoat Head (**Fig. 3A**; Leleu et al., 2010). Floodplain deposits at Economy Point are thicker than in the
218 southern shore sections and are interpreted to represent a more distal equivalent to the distributive fluvial
219 system (e.g. Hartley et al. 2010; Weissmann et al., 2010) that had been documented in the south of the Minas
220 sub-basin (Leleu et al., 2009).

221

222 The location of the Economy Point section immediately adjacent to the CCFZ together with the north- to
223 north-eastwards palaeoflow indicators suggests that the Cobequid High did not deflect drainage during middle
224 Wolfville deposition. In addition, the absence of angular, coarse-grained first-cycle, northerly derived material
225 indicates that the rift basin extended north of the present-day northern margin of the Minas sub-basin and was
226 dominated by a transverse fluvial system flowing northward. These observations do not necessarily mean that
227 the CCFZ was not active, but they do indicate that it had no significant syn-depositional topography if
228 sedimentation rate compensated vertical tectonic displacement (sediments filled accommodation space formed
229 by subsidence).

230

231 **Soley Cove – Red Head section**

232 The Soley Cove section is located 6 km west of the Economy Point section (**Fig.3B**) and is laterally equivalent
233 to the Red Head section cropping out further west. Between Soley Cove and Red Head (over 4 kilometres),
234 the outcrops are continuous and show very thick packages of alluvial-fan deposits interbedded with aeolian
235 deposits up to 10 m in thickness (Hubert & Mertz, 1980; **Figs. 5O, 8**). The rocks are exposed along sea cliffs
236 that are up to 30 metres high and close to vertical. The cliffs are densely faulted hampering detailed logging
237 and correlation. However, since displacement on each fault is limited, an estimation of lateral variation of
238 Alluvial-Fan and Aeolian facies associations was possible (**Fig. 8**).

239

240 The Soley Cove section comprises very angular alluvial-fan sediments that grade into finer-grained fan and
241 playa-margin deposits (**Table 1**). Aeolian facies accounts for <1% of the succession in this section; however
242 they are very abundant (approx. 85%) to the west along the cliff between Soley Cove and Red Head. The

243 Soley Cove – Red Head transect comprises mainly alluvial-fan clast-supported breccia, matrix-supported
244 breccia and pebbly sandstones (deposited by debris flow, hyperconcentrated flow and fluvial processes; **Table**
245 **1**). Clasts are very angular and locally derived from basement rocks (meta-granite and diorite and meta-
246 sediments). Aeolian sand was reworked to form part of the matrix to the breccia and pebbly sandstones. The
247 top of the section displays playa-margin facies association considered typical of the Blomidon Formation in
248 particular with the occurrence of the sandpatch fabric sandstones. At Soley Cove, the lowermost part of the
249 section (**Fig. 6**) contains thick packages of coarse alluvial-fan deposits (clast- and matrix- supported breccia
250 and pebbly sandstones), locally interbedded with thin playa-margin beds, passing upwards into dominantly
251 playa-margin facies. The uppermost part of the section displays thick distal-fan deposits (granule-bearing
252 sandstones and ripple-laminated sandstones) interbedded with sandpatch sandstones and claystones
253 punctuated by thin, coarse alluvial-fan deposits.

254

255 The relative volume of preserved aeolian deposits (from 1% to 50 % and then to 85% of exposure) increases
256 to the west, whilst the amount of alluvial-fan deposits decreases (**Fig. 8**). Aeolian-dune deposits preserved
257 close to Soley Cove are up to 8 m thick, while the westernmost aeolian beds close to Red Head form a
258 composite aeolian package up to 27 m thick with the thickest individual aeolian bed of 4 metres. Thickness of
259 alluvial-fan beds varies from 1 to 3 m but variations are not organised in a preferential direction. However
260 aeolian beds are more frequently punctuated by fan deposits towards the east (Soley Cove where they
261 dominate largely) and the volume of alluvial-fan sediments overall decreases to the west (**Fig. 8**).

262

263 **Correlation across the Minas sub-basin**

264 The base of the Blomidon Formation crops out north of the Medford section (in SW Minas sub-basin) and at
265 Soley Cove, on the northern side of the present-day Minas sub-basin (**Fig. 3A**). At Medford the Wolfville/
266 Blomidon boundary is marked by the cessation of confined channelized fluvial deposits and the dominance of
267 sheetflood and playa deposits forming the Playa-Margin facies association (Leleu & Hartley, 2010).

268 Deposition of numerous fined-grained unconfined flows occurred and shallow lakes developed occasionally in
269 the area but eventually dried up as indicated by aeolian adhesion ripples on the wet surface. Aeolian dunes are

270 preserved beneath the lowermost Blomidon Formation at the Medford section where the last aeolian bed is
271 recorded in the southern stratigraphy (11 meters above the contact with the upper Wolfville Formation; **Fig.**
272 **9**). In the northern sections (Soley Cove-Red Head section) aeolian dunes were replaced progressively by
273 alluvial-fan and playa sedimentation to the east (**Fig. 10**). Consequently playa-margin deposits are the
274 predominant facies in the south (Medford section) with playa and shallow-lake deposits dominating the
275 northern stratigraphy (Gould, 2001) as unconfined flows from the fans decreased progressively in grain size
276 and eventually stopped. Typically lithofacies distribution changes significantly across the basin and estimating
277 an age for the aeolian and alluvial-fan deposits is not straightforward, and consequently direct
278 lithostratigraphic correlation cannot be used. However we have used the termination of channelized fluvial
279 deposition and the occurrence of specific playa deposits to define the boundary between Wolfville and
280 Blomidon Fm (Leleu & Hartley, 201), we also suggest using the termination of aeolian deposition across the
281 basin as recording a new phase in the basin fill. Indeed aeolian deposits are not present in the uppermost
282 stratigraphy and can be considered a marker for a change in the basin stratigraphy. We suggest therefore that
283 aeolian dune and alluvial-fan deposits may also represent the lowermost Blomidon Formation and older
284 deposits in the northern sections. Whilst this approach cannot be considered accurate from a
285 chronostratigraphic perspective, it is based on the idea of correlating basin-wide changes in facies that reflect
286 climatic variability, an approach that has been used previously in arid continental successions (e.g. George &
287 Berry 1993).

288

289 **DRAINAGE EVOLUTION**

290 The tectono-sedimentary linkage between the Minas and the Chignecto sub-basins and the amount and timing
291 of displacement along the CCFZ are not well understood. Here we summarise the temporal development of
292 the structure based on the sedimentary record (i.e. facies distribution, architecture and palaeoflow) (**Fig. 11**).

293

294 **Carnian:** During Carnian times, fluvial deposits of the Wolfville Formation started to be preserved in the
295 southern Minas area, corresponding to a major period of basin enlargement (Leleu & Hartley, 2010). These
296 fluvial systems flowed northwards from the southern rift shoulder uplands into the Minas sub-basin. They

297 formed transverse fluvial systems that were either connected to an axial trunk river in the Fundy and
298 Chignecto sub-basins or terminated in a playa basin (**Fig. 11A**). The fluvial palaeoflows measured in the
299 southern Minas sub-basin indicate that the fluvial system was flowing to the NE (means between N019° and
300 N051°). At Economy Point, located about 8 kilometres downstream, the mean palaeocurrent direction of the
301 flow is to N068°. The range of palaeoflows presents a similar fluvial direction to the NE. It is likely that the
302 Cobequid High was not present at the time although one could argue that there is a little change in direction
303 that could reflect a slight deviation of the fluvial system. So it is most likely that there was no major
304 topography along the CCFZ prior to latest Wolfville or earliest Blomidon deposition but it is possible that a
305 local change in subsidence related to CCFZ activity might have influenced the main river path.

306

307 **Early Norian:** Less data are available on the transition between the Wolfville and Blomidon Formations
308 during early Norian times (Olsen et al., 2005). In the southwest Minas sub-basin sections, fluvial systems
309 were smaller and terminal, comprising feeder channels, terminal splay and mudflat deposits (Leleu and
310 Hartley, 2010). On the northern side of the Minas sub-basin, aeolian sediments were abundant at that time and
311 aeolian deposits are locally thick (Red Head section in the Minas sub-basin; Hubert & Mertz, 1984).
312 Simultaneously, the development of alluvial fans implied that the Cobequid highlands formed an intra-basinal
313 high and sourced the alluvial-fan deposits (**Fig. 11B**). In consideration of the amount of polished quartz sand
314 of aeolian origin within the fan successions, it is likely that aeolian sand was reworked as the matrix for
315 debris-flow processes suggesting that aeolian dunes or sand were also present on the top of the horst structure.

316

317 **Mid Norian-Rhaetian** During early Blomidon deposition, only a few aeolian deposits are preserved and
318 eventually no aeolian deposits are preserved at all later in the Blomidon Formation (late Norian and Rhaetian)
319 (**Fig. 11C**). The Fundy and Minas sub-basins are dominated by splay and shallow-lake deposits and become
320 increasingly evaporitic at some stratigraphic intervals, attesting to periods of more intense evaporation. The
321 playa-lake system was very extensive across the entire Fundy Basin and the Cobequid High might have
322 already been buried as no alluvial-fan deposits are recorded in the upper part of the Blomidon Formation
323 along the CCFZ. Channel-fill deposits are located along the southern shore of the Minas and Fundy sub-basins

324 (Gould, 2001; Leleu & Hartley, 2010) and we suggest therefore that, although relatively minor, the main
325 fluvial systems feeding the basin were sourced from the south.

326

327 **DISCUSSION**

328 **Drainage and intra-basinal faulting in the Fundy rift basin**

329 Previous models of drainage development in the Minas sub-basin considered the Cobequid High as a long-
330 lived structure in the Fundy basin with rivers flowing northwards from the rift shoulder and southwards from a
331 long-lived horst structure across the Minas sub-basin and being deflected to the east to join a major trunk river
332 system (Hubert and Mertz, 1984; Hubert & Forlenza, 1988). Here, we demonstrate however that the Cobequid
333 High was not developed as a topographic high during deposition of the lower and middle Wolfville Fm, and
334 most likely not present prior to then either (Leleu & Hartley, 2010). The presence of the intrabasinal CCFZ
335 has major implications for the drainage organization in the basin history. The sedimentary architecture is
336 complex along the CCFZ where deposits are highly faulted, but the assessment of facies distribution and
337 palaeoflow reconstruction within a stratigraphic framework provide evidence for the timing of uplift of an
338 intrabasinal topographic high by the CCFZ. Growth strata were reported along the CCFZ (Withjack et al.
339 2010), but it is clear that topography was created only during Norian times, when alluvial-fan deposition
340 commenced. The earlier phase of sedimentation in the Minas sub-basin shows a fluvial system flowing
341 consistently to the northeast suggesting the absence of a topographic high. Thus despite the existence of
342 growth strata along the CCFZ, the absence of marked topography prior to alluvial-fan sedimentation means
343 that fluvial sedimentation rate compensated for the accommodation space created by local tectonics. A major
344 tectonic event created the horst structure which fed alluvial fans at some point in the basin stratigraphy
345 (estimated during the early Norian). The stratigraphy close to the CCFZ shows that alluvial fans aggraded
346 through time before retrograding and finally disappeared. Fine-grained lacustrine/ playa deposits were then
347 dominant in the whole basin and even close to the CCFZ. This suggests that the horst structure became buried
348 by the Blomidon low-energy lacustrine/ playa deposits. As the sedimentation rate for the Blomidon Fm is
349 particularly low (200 meters in the Minas sub-basin for 15 My), it is likely that there was no more vertical

350 displacement along the CCFZ and that most growth strata imaged in seismic line belong to the Wolfville
351 Formation and the base of the Blomidon Formation.

352

353 **Aeolian bed preservation within fluvial deposits**

354 Aeolian sediments are well preserved in the upper Wolfville Fm and at the transition into the lowermost
355 Blomidon. From south to north the preservation of aeolian facies increases towards the CCFZ. Preservation of
356 aeolian beds implies that sediments were buried beneath a regional base-level that normally equates to the
357 groundwater table in aeolian successions (Koçurek & Havholm, 1993). This occurs either through subsidence
358 and subsequent relative rise in groundwater table or by an absolute rise in water table following a change in
359 climate (Koçurek 1981; Mountney et al., 1999). The most obvious mechanism for aeolian bed preservation in
360 this case is tectonic subsidence as preserved thickness increase towards the CCFZ and thins to the south. In
361 addition, aeolian beds are interbedded with alluvial-fan deposits indicating activity on the CCFZ. Therefore
362 the combination of fan deposition and preservation of aeolian deposits seems to indicate that vertical
363 movement along the CCFZ accelerated around the early Norian. In the southern margin of the Minas sub-
364 basin, preserved aeolian beds are thin (2 meters) and intercalated with either fluvial sandstone or lacustrine
365 mudstones punctuated by exposure surfaces with desiccation cracks (Leleu & Hartley, 2010). There is no
366 indication of an elevated groundwater level in the basin such as adhesion ripples or wavy laminated sandstone
367 (Koçurek, 1981) until upper units within the basin stratigraphy (Blomidon Fm). Interestingly, no aeolian beds
368 are preserved higher in the stratigraphy, i.e. in Blomidon Fm, when a high water-table is recorded by adhesion
369 ripples (with sand-patch fabric). Thus preservation of both the intercalated aeolian sediments and alluvial-fan
370 deposits corroborate an increase in activity of the CCFZ during deposition in the basin and no absolute higher
371 water-table associated with a change in climatic regime. This interpretation supports the idea that the
372 development of a wide lacustrine rift basin (with little fluvial input) following the deposition of large fluvial
373 systems in the rift basin is not climatically driven. The decrease in sediment supply in the fluvial systems has
374 been interpreted to reflect a decrease in fluvial gradient due to progressive erosion through time and no
375 rejuvenation of rift-shoulder relief (Smoot 1991; Leleu & Hartley 2010) possibly related to a decrease in
376 tectonic activity (final phase of Triassic rifting). Nevertheless, growth structures along the main boundary

377 faults of the Fundy Basin attest that rifting was still active and large-scale tectonics occurred in the Central
378 Atlantic domain.

379 In summary, the CCFZ segmented the initial large rift basin and formed an intrabasinal horst that fed the
380 alluvial fans. The accumulation and preservation of aeolian dunes adjacent to the fault scarp along the
381 Cobequid High, especially to the west of the study area, were probably favoured by fault-induced subsidence.
382 Accumulation of aeolian dunes mainly south of the Cobequid high and close to the fault scarp suggests that
383 either the horst represented a topographic barrier to aeolian dunes or formed a wind shadow that favoured
384 local accumulation of aeolian sands. The mean palaeowind is to the SE and therefore it is more likely that the
385 Cobequid High acted as a wind shadow. This interpretation is consistent with the presence of windblown sand
386 in the fan catchment that was reworked by floods to form the matrix of debris flows and fluvial pebbly
387 sandstones. The occurrence of synchronous alluvial-fan and aeolian deposits validates the development of the
388 northern topographic high prior to deposition.

389

390 **CONCLUSIONS**

391 The facies types, distribution and palaeoflow data from Upper Triassic alluvial and aeolian deposits in the
392 Fundy Basin along the CCFZ are used to determine timing of fault activity and suggest that an initially large
393 Carnian rift basin was segmented by an intrabasinal horst during Norian times. A Carnian transverse fluvial
394 system flowing to NE does not show major diversion and suggests that no topographic high was present at
395 that time. Alluvial-fan deposits intercalated upwards with typical Norian playa deposits recorded the
396 development of the intrabasinal horst. Fining-upward fan deposits and development of fine-grained playa
397 successions suggest that topography was not renewed and was eventually buried by sediment aggradation
398 within the basin. Simultaneous with alluvial-fan development, aeolian dunes were preserved adjacent to the
399 CCFZ. Aeolian accumulation was probably accentuated due to the fault scarp acting as a wind shadow with
400 preservation of aeolian deposits promoted by subsidence beneath a regional erosional base level.

401

402 Alluvial-fan deposits were sourced from local relief of the intrabasinal horst with very angular clasts
403 transported mainly by debris and hyperconcentrated flows. Some of the fans forming the CCFZ piedmont

404 flowed through the dune field mainly located to the west. Aeolian sands form a large fraction of the matrix for
405 coarse-grained fan deposits, indicating that windblown sand was trapped onto the proximal domains of the fan
406 or within the fan catchments before being remobilised by alluvial processes.

407

408 **ACKNOWLEDGMENTS**

409 The authors would like to acknowledge Shell E and P for funding this study, Rob Raeside at the Acadia
410 University and Liz Kusters for their support during the field seasons. We also would like to thank Brian P. J.
411 Williams for enthusiastic discussions in the field.

412

413 **REFERENCES**

- 414 Ackermann, R.V., Schlische, R.W. & Olsen, P.E. 1995. Synsedimentary collapse of portions of the lower
415 Blomidon Formation (Late Triassic), Fundy rift basin, Nova Scotia. *Canadian Journal of Earth Sciences*,
416 **32**, 1965-1976.
- 417 Allen, J.R.L. 1982. *Sedimentary structures: their character and Physical Basis, Volume 1*. Amsterdam,
418 Elsevier Science Publishers, Developments in Sedimentology, **30**, 611 p.
- 419 Best, J.L. & Bridge, J.S. 1992. The morphology and dynamics of low-amplitude bedwaves upon upper stage
420 plane beds, and the preservation of planar laminae. *Sedimentology*, **39**, 737-752.
- 421 Best, J.L., Ashworth, P.J., Bristow, C.S. & Roden, J. 2003. Three-dimensional sedimentary architecture of a
422 large, mid-channel sand braid bar, Jamuna River, Bangladesh. *Journal of Sedimentary Research*, **73**, 516-
423 530.
- 424 Blair, T.C. 2000. Sedimentology and progressive tectonic unconformities of the sheetflood-dominated Hell's
425 Gate alluvial fan, Death Valley, California. *Sedimentary Geology*, **132**, 233-262.
- 426 Blair, T.C. & McPherson, J.G. 1994a. Alluvial fans and their natural distinction from rivers based on
427 morphology, hydraulic processes, sedimentary processes, and facies assemblages. *Journal of Sedimentary*
428 *Research*, **A64**, 450-489.
- 429 Blair, T.C. & McPherson, J.G. 1998. Recent debris flow processes and resultant form and facies of the
430 Dolomite alluvial fan, Owens Valley, California. *Journal of Sedimentary Research*, **68**, 800-818.
- 431 Bridge, J.S. 2003. *Rivers and floodplains; forms, processes, and sedimentary record*. Oxford, United
432 Kingdom, Blackwell Publishing, 491 p.
- 433 Bridge, J.S. & Leeder, M.R. 1979. A simulation model of alluvial stratigraphy. *Sedimentology*, **26**, 617-644.
- 434 Bridge, J.S. & Tye, R.S. 2000. Interpreting the dimensions of ancient fluvial channel bars, channels, and
435 channel belts from wireline-logs and cores. *American Association of Petroleum Geologists Bulletin*, **84**,
436 1205-1228.
- 437 Brookfield, M.E., 1977. The origin of bounding surfaces in ancient aeolian sandstones. *Sedimentology*, **24**,
438 303-332.

- 439 Cirilli, S., Marzoli, A., Tanner, L.H., Bertrand, H., Buratti, N., Jourdan, F., Bellieni, G., Kontak, D.J. & Renne,
440 P.R. 2009. Latest Triassic onset of the Central Magmatic Province (CAMP) volcanism in the Fundy Basin
441 (Nova Scotia). New stratigraphic constraints. *Earth and Planetary Science Letters*, **286**, 514-525.
- 442 Cornet, B. 1977. *The palynostratigraphy and age of the Newark Supergroup*. PhD Thesis, PA, USA,
443 Pennsylvania State University, University Park, 527p.
- 444 Coussot, P. & Meunier, M. 1996. Recognition, classification and mechanical description of debris flows.
445 *Earth Science Review*, **40**, 209-227.
- 446 Coussot, P. & Ansey, C. 1999. Rheophysical classification of concentrated suspensions and granular pastes.
447 *Physical Review*, **E59**, 4445-4457.
- 448 Deenen, M.H.L., Ruhl, M., Bonis, N.R., Krijgsman, W., Kuerschner, W.M., Reitsma, M. & Van Bergen, M.J.
449 2010. A new chronology for the end-Triassic mass extinction. *Earth and Planetary Science Letters*, **291**,
450 113-125.
- 451 Fisher, J.A., Nichols, G. J. & Waltham, D. A. 2007. Unconfined flow deposits in distal sectors of fluvial
452 distributary systems; examples from the Miocene Luna and Huesca systems, northern Spain. *Sedimentary*
453 *Geology*, **195**, 55-73.
- 454 Fowell, S.J., & Traverse, A. 1995. Palynology and age of the upper Blomidon Formation, Fundy Basin, Nova
455 Scotia. *Review of Palaeobotany and Palynology*, **86**, 211-233.
- 456 George, G. T., & Berry, J. K., 1993. A new lithostratigraphy and depositional model for the Upper Rotliegend
457 of the UK sector of the southern North Sea. In North, C. P., and Prosser, D. J., eds. Characterization of
458 fluvial and aeolian reservoirs. *Geological Society Special Publications*, **73**, 291–319.
- 459 Gould, S. 2001. *Integrated sedimentological and whole-rock trace element geochemical correlation of*
460 *alluvial red-bed sequences at outcrop and in the subsurface*. PhD thesis, Aberdeen, UK, University of
461 Aberdeen, 278 p.
- 462 Hartley, A.J., Weissmann, G.S., Nichols, G.D. & Warwick, G.L. 2010. Distributive fluvial systems:
463 characteristics, distribution and controls on development. *Journal of Sedimentary Research*, **80**, 167-183.
- 464 Hubert, J.F. & Mertz, K.A., JR. 1980. Eolian dune field of Late Triassic age, Fundy Basin, Nova Scotia.
465 *Geology*, **8**, 516-519.
- 466 Hubert, J.F. & Hyde, M.G. 1982. Sheet-flow deposits of graded beds and mudstones on an alluvial sandflat -
467 playa system: Upper Triassic Blomidon redbeds, St. Mary's Bay, Nova Scotia. *Sedimentology*, **29**, 457-
468 474.
- 469 Hubert, J.F. & Mertz, K.A., JR. 1984. Eolian sandstones in Upper Triassic-Lower Jurassic red beds of the
470 Fundy Basin, Nova Scotia. *Journal of Sedimentary Petrology*, **54**, 798-810.
- 471 Hubert, J.F. & Forlenza, M.F. 1988. Sedimentology of braided-river deposits in Upper Triassic Wolfville
472 redbeds, southern shore of Cobequid Bay, Nova Scotia. *Developments in Geotectonics*, **22**, 231-237.
- 473 Hunter, R.E. 1973. Pseudo-crosslamination formed by climbing adhesion ripples. *Journal of Sedimentary*
474 *Petrology*, **43**, 1125-1127.
- 475 Hunter, R.E. 1977. Basic types of stratification in small eolian dunes. *Sedimentology*, **24**, 361-387.
- 476 Kent, D.V. & Olsen, P.E. 2000. Magnetic polarity stratigraphy and paleolatitude of the Triassic - Jurassic
477 Blomidon Formation in the Fundy Basin (Canada): implications for early Mesozoic tropical climate
478 gradients. *Earth and Planetary Science Letters*, **179**, 311-324.
- 479 Kent, D.V. & Tauxe, L. 2005. Corrected Late Triassic latitudes for continents adjacent to the North Atlantic.
480 *Science*, **307**, 240-244.
- 481 Klein, G.d. 1962. Triassic sedimentation, Maritime Provinces, Canada. *Geological Society of America*
482 *Bulletin*, **73**, 1127-1145.

- 483 Koçurek, G. 1981. Significance of interdune deposits and bounding surfaces in aeolian dune sands.
484 *Sedimentology*, **28**, 753–780.
- 485 Koçurek, G., 1988. First-order and super bounding surfaces in eolian sequences—bounding surfaces revisited.
486 *Sedimentary Geology*, **56**, 193–206.
- 487 Kocurek, G. & Fielder, G. 1982. Adhesion structures. *Journal of Sedimentary Petrology*, **52**, 1229-1241.
- 488 Koçurek, G. & Havholm, K.G.1993. Eolian sequence stratigraphy – A conceptual framework. In Weimer, P.
489 & Posamentier, H.W. (eds) *Siliciclastic sequence stratigraphy*, American Association of Petroleum
490 Geologists Memoirs, **58**, 393-409.
- 491 Kontak, D. J. 2008. On the edge of CAMP: Geology and volcanology of the Jurassic North Mountain Basalt,
492 Nova Scotia. *Lithos*, **101**, 74-101.
- 493 Leleu, S. & Hartley, A.J. 2010. Controls on the stratigraphic development of the Triassic Fundy Basin, Nova
494 Scotia: implications for the tectono-stratigraphic evolution of Triassic Atlantic rift basins. *Geological*
495 *Society of London, Journal*, **167**, 437-454.
- 496 Leleu, S., Hartley, A. J. & Williams, B.P.J. 2009. Large-scale alluvial architecture and correlation in a Triassic
497 pebbly braided river system, lower Wolfville Formation (Fundy Basin, Nova Scotia, Canada). *Journal of*
498 *Sedimentary Research*, **79**, 265-286.
- 499 Leleu, S., van Lanen, X. M. & Hartley, A. J. 2010. Controls on the architecture of a Triassic sandy fluvial
500 system, Wolfville Formation, Fundy Basin, Nova Scotia, Canada: Implications for the interpretation and
501 correlation of ancient fluvial successions. *Journal of Sedimentary Research*, **80**, 867-883.
- 502 Lowe, D.R. 1982. Sediment gravity flows ; II, Depositional models with special reference to the deposits of
503 high density turbidity currents. *Journal of Sedimentary Petrology*, **52**, 279-297.
- 504 Lucas, S. G. & Tanner, L.H. 2007. The nonmarine Triassic-Jurassic boundary in the Newark Supergroup of
505 eastern North America. *Earth Science Reviews*, **84**, 1-20.
- 506 Lunt, I.A., Bridge, J.S. & Tye, R.S. 2004. A quantitative, three-dimensional depositional model of gravelly
507 braided rivers. *Sedimentology*, **51**, 377-414.
- 508 Marzoli, A., Renne, P.R., Ernesto, M., Bellieni, G. & De Min, A. 1999.Extensive 200-million-year-old
509 continental flood basalts of the Central Atlantic Magmatic Province. *Science*, **284**, 616-618.
- 510 McHone, J.G. 2000. Non-plume magmatism and rifting during the opening of the central Atlantic Ocean.
511 *Tectonophysics*, **316**, 287-296.
- 512 Mertz, K.A. & Hubert, J.F. 1990. Cycles of sand-flat sandstone and playa-mudstone in the Triassic - Jurassic
513 Blomidon redbeds, Fundy rift basin, Nova Scotia: implications for tectonic and climatic controls.
514 *Canadian Journal of Earth Sciences*, **27**, 442-451.
- 515 Miall, A.D. 1996. *The Geology of Fluvial Deposits; Sedimentary Facies, Basin Analysis, and Petroleum*
516 *Geology*. New York, Springer-Verlag, 582 p.
- 517 Mountney, N., Howell, J., Flint, S. & Jerram, D. 1999. Climate, sediment supply and tectonics as controls on
518 the deposition and preservation of the aeolian-fluvial Etjo Sandstone Formation, Namibia. *Geological*
519 *Society of London, Journal*, **156**, 771-777.
- 520 Nadon, G.C. & Middleton, G.V. 1984. Tectonic control of Triassic sedimentation in southern New
521 Brunswick; local and regional implications. *Geology*, **12**, 619-622.
- 522 Nadon, G.C. & Middleton, G.V. 1985.The stratigraphy and sedimentology of the Fundy Group (Triassic) of
523 the St. Martins area, New Brunswick. *Canadian Journal of Earth Sciences*, **22**, 1183-1203.
- 524 Nichols, G.J. & Fisher, J.A. 2007. Processes, facies and architecture of fluvial distributary system deposits.
525 *Sedimentary Geology*, **195**, 75-90.

- 526 Ogg, J.G., Ogg, G. & Gradstein, F.M. 2008. *The concise geologic time scale*. NY, USA, Cambridge
527 University Press, 177p.
- 528 Olsen, P.E. 1986. A 40-million-year lake record of early Mesozoic orbital climatic forcing. *Science*, **234**, 842-
529 848.
- 530 Olsen, P.E. 1990. Tectonic, climatic, and biotic modulation of lacustrine ecosystems: examples from Newark
531 Supergroup of eastern North America. Lacustrine basin exploration; case studies and modern analogs.
532 *American Association of Petroleum Geologists Memoir*, **50**, 209-224.
- 533 Olsen, P.E.. 1997. Stratigraphic record of the early Mesozoic breakup of Pangea in the Laurasia - Gondwana
534 rift system. *Annual Review of Earth and Planetary Sciences*, **25**, 337-401.
- 535 Olsen, P.E., and Kent, D.V., 1996, Milankovitch climate forcing in the tropics of Pangaea during the Late
536 Triassic. *Palaeogeography, Palaeoclimatology, Palaeoecology*, **122**, 1-26.
- 537 Olsen, P.E. & Schlische, R.W. 1990. Transtensional arm of the early Mesozoic Fundy rift basin;
538 penecontemporaneous faulting and sedimentation. *Geology*, **18**, 695-698.
- 539 Olsen, P.E. & Sues, H.D. 1986. Correlation of continental Late Triassic and Early Jurassic sediments and
540 patterns of the Triassic-Jurassic tetrapod transition. In Padian, K. (ed) *The beginning of the age of*
541 *dinosaurs; faunal change across the Triassic-Jurassic boundary*. Cambridge University Press, UK, 321-
542 351.
- 543 Olsen, P.E., Schlische, R.W. & Gore, P.J.W. 1989. Newark Basin, Pennsylvania and New Jersey; Stratigraphy.
544 In International Geological Congress, 28th, Field Trip Guidebook T351: Washington, DC, American
545 Geophysical Union, 183 p.
- 546 Olsen, P.E., Kent, D.V., Fowell, S.J., Schlische, R.W., Withjack, M.O. & LeTourneau, P.M. 2000.
547 Implications of a comparison of the stratigraphy and depositional environments of the Argana (Morocco)
548 and Fundy (Nova Scotia, Canada) Permian-Jurassic basins. In Oujidi, M. & El-Touhami, M. (eds) *Le*
549 *Permien et le Trias du Maroc*. Actes de la Première Réunion du Groupe Marocain du Permian et du Trias,
550 165-183.
- 551 Olsen, P.E., Koeberl, C., Huber, H. Montanari, A., Fowell, S. J., Et-Touhami, M. & Kent, D. V. 2002.
552 Continental Triassic-Jurassic boundary in central Pangea; recent progress and discussion of an Ir anomaly.
553 *Geological Society of America Special Paper*, **356**, 505-522.
- 554 Paik, I.S. & Kim, H.J. 2006. Playa lake and sheetflood deposits of the Upper Cretaceous Jindong Formation,
555 Korea; occurrences and palaeoenvironments. *Sedimentary Geology*, **187**, 83-103.
- 556 Postma, G. 1986. Classification for sediment gravity flow deposits based on flow conditions during
557 sedimentation. *Geology*, **14**, 291-294.
- 558 Rodine, J.D. & Johnson, A.M. 1976. The ability of debris, heavily freighted with coarse clastic materials, to
559 flow on gentle slopes. *Sedimentology*, **23**, 213-234.
- 560 Schlische, R.W. 1993. Anatomy and evolution of the Triassic-Jurassic continental rift system, eastern North
561 America. *Tectonics*, **12**, 1026-1042.
- 562 Schlische, R.W. & Olsen, P.E. 1990. Quantitative filling models for continental extensional basins with
563 applications to the early Mesozoic rifts of eastern North America. *Journal of Geology*, **98**, 135-155.
- 564 Smoot, J.P. 1983. Depositional subenvironments in an arid closed basin; the Wilkins Peak Member of the
565 Green River Formation (Eocene), Wyoming, USA. *Sedimentology*, **30**, 801-827.
- 566 Smoot, J.P. 1991. Sedimentary facies and depositional environments of early Mesozoic Newark Supergroup
567 basins, eastern North America. *Palaeogeography, Palaeoclimatology, Palaeoecology*, **84**, 369-423.
- 568 Stear, W.M. 1983. Morphological characteristics of ephemeral stream channel and overbank splay sandstone
569 bodies in the Permian Lower Beaufort Group, Karoo Basin, South Africa. In Collinson, J. D. & Lewin, J.

- 570 (eds) *Modern and ancient fluvial systems*. International Association of Sedimentologists, Special
571 Publication, **6**, 405-420.
- 572 Steel, R.J. & Thompson, D.B. 1983. Structures and textures in Triassic braided stream conglomerates ('Bunter'
573 pebble beds) in the Sherwood Sandstone Group, North Staffordshire, England. *Sedimentology*, **30**, 341-
574 367.
- 575 Tanner, L.H. 1993. Pedogenic features of the Triassic-Jurassic Fundy Group, Fundy Basin, Nova Scotia, *In*
576 *Proceedings, Geological Society of America, Annual meeting*, **25**, 69.
- 577 Tanner, L.H. 2000. Triassic-Jurassic lacustrine deposition in the Fundy rift basin, Eastern Canada. *American*
578 *Association of Petroleum Geologists, Studies in Geology*, **46**, 159-166.
- 579 Tanner, L.H. & Kyte, F.T. 2005. Anomalous iridium enrichment at the Triassic-Jurassic boundary, Blomidon
580 Formation, Fundy Basin, Canada. *Earth and Planetary Science Letters*, **240**, 634-641.
- 581 Tanner, L.H., Lucas, S.G. & Chapman, M.G. 2004. Assessing the record and causes of Late Triassic
582 extinctions. *Earth Science Reviews*, **65**, 103-139.
- 583 Vallance, J.W. 2000. Lahars. *In* : Sigurdsson H., Houghton B.F., McNutt S.R., Rymer H. et Stix J. (eds)
584 *Encyclopedia of volcanoes*. Academic Press, San Diego, USA, 601-616.
- 585 Wade, J.A., Brown, D.E., Traverse, A. & Fensome, R.A. 1996. The Triassic - Jurassic Fundy Basin, eastern
586 Canada: Regional setting, stratigraphy and hydrocarbon potential. *Atlantic Geology*, **32**, 189-231.
- 587 Weissmann, G.S., Hartley, A.J., Nichols, G.J., Scuderi, L.A., Olson, M., Buehler, H. & Banteah, R. 2010.
588 Fluvial form in modern continental sedimentary basins. *Geology*, **38**, 39-42.
- 589 Welsink, H.J., Dwyer, J.D. & Knight, R.J. 1989. Tectono-stratigraphy of the passive margin off Nova Scotia.
590 *In* Tankard, A. J. & Balkwill, H. R, eds, *Extensional tectonics and stratigraphy of the North Atlantic*
591 *margins. American Association of Petroleum Geologists, Memoir*, **46**, 215-231.
- 592 Whiteside, J. H., Olsen, P.E., Kent, D.V., Fowell, S. J. & Et-Touhami, M. 2007. Synchrony between the
593 Central Atlantic Magmatic Province and the Triassic-Jurassic mass-extinction event?. *Palaeogeography,*
594 *Palaeoclimatology, Palaeoecology*, **244**, 345-367.
- 595 Withjack, M.O., Olsen, P.E. & Schlische, R.W. 1995. Tectonic evolution of the Fundy Rift Basin, Canada -
596 evidence of extension and shortening during passive margin development. *Tectonics*, **14**, 390-405.
- 597 Withjack, M.O., Schlische, R.W. & Olsen, P.E. 1998. Diachronous rifting, drifting, and inversion on the
598 passive margin of central eastern North America: an analog for other passive margins. *American*
599 *Association of Petroleum Geologists Bulletin*, **82**, 817-835.
- 600 Withjack, M.O., Schlische, R.W. & Olsen, P.E. 2002. Rift-basin structure and its influence on sedimentary
601 systems, *in* Renaut, R.W. and Ashley, G.M., eds, *Sedimentation in continental rifts*. Special Publication -
602 *Society for Sedimentary Geology*, **73**, 57-81.
- 603 Withjack. M.O., Schlische, R.W. & Baum, M.S. 2009. Extensional development of the Fundy rift basin,
604 southeastern Canada. *Geological Journal*, **44**, 631-651.
- 605 Withjack. M.O., Baum, M.S. & Schlische, R.W. 2010. Influence of preexisting fault fabric on inversion-
606 related deformation: a case study of the inverted Fundy rift basin, southeastern Canada. *Tectonics*, **29**,
607 TC6004, doi:10.1029/2010TC002744.

608

609 LIST OF FIGURES

- 610 **Figure 1:** Introduction to the Fundy Basin; (A) Map of the Fundy Basin showing sub-basins, major faults
611 (modified from Wade et al., 1996) and location of cross-sections: (B) Cross-section of the Chignecto and

612 Minas sub-basins showing growth-structures along major faults (after Withjack et al., 2010; line 82-37); (C)
613 Cross-section of the western Minas sub-basin (after Withjack et al., 2010; line 82-28); (D) Interpreted
614 geological cross-section of the Minas sub-basin supported by seismic data (after Withjack et al., 2010);
615 **Figure 2:** Stratigraphy of the Red Beds in the Fundy Basin (Nadon and Middleton, 1984; Olsen, 1997; Olsen
616 et al., 2005; Lucas and Tanner, 2007; Cirilli et al., 2009). Time-scale from Ogg et al., 2008.

617
618 **Figure 3:** (A) Geological map of the Minas sub-basin and location of the main Triassic sections in bold; (B)
619 Detailed map (modified after Olsen & Schlische, 1990) of the fault complex showing the studied sections.

620
621 **Figure 4:** Composite lithostratigraphy of the Minas sub-basin (after Leleu and Hartley, 2010); (A) lower
622 Wolfville Formation (coarse-grained fluvial succession) overlain by (B) middle Wolfville Formation (fine-
623 grained fluvial succession) and (C) upper Wolfville Formation, comprising fluvial, ephemeral-fluvial,
624 lacustrine and aeolian sediments. Transition between middle and upper Wolfville Formation is not exposed;
625 The Wolfville Formation is overlain by the (D) Blomidon Formation comprising mainly mudstones and
626 occasional tabular sand-sheets. The extrusive North Mountain Basalt overlies the Blomidon Formation.

627
628 **Figure 5:** Lithofacies examples: (A) clast-to-matrix supported breccia showing a chaotic and poorly sorted
629 fabric (*lithofacies 1*) overlain by pebbly sandstones (*lithofacies 3*); (B) horizontal beds of clast-supported
630 breccia (*lithofacies 1*), the basal bed is normally graded, the bed in the center is inversely graded with an
631 intercalated 15-cm-thick bed of matrix-supported breccia (*lithofacies 2*); (C) thick basal matrix-supported
632 breccia (*lithofacies 1*) overlain a by 30-cm-thick, weakly erosive clast-supported breccia (*lithofacies 1*) and
633 intercalated with thin beds of clast-supported and matrix-supported breccia, clast-supported breccias show
634 long-axis imbrication (flow to the left); (D) very thin beds (< 10cm) of intercalated clast-supported and
635 matrix-supported breccias, clast-supported breccias show long-axis imbrication (flow to the right); (E) thick
636 matrix-supported breccia (*lithofacies 2*) overlain by pebbly sandstones showing horizontal bedding
637 (*lithofacies 3*); (F) close-up showing coarse well-rounded (white) grains forming the matrix of alluvial-fan
638 deposits. The coarse grains are of aeolian origin; (G) amalgamated beds of granule-bearing sandstones

639 (*lithofacies 4*). Beds are 3 cm thick and slightly erosive with thin pebble lags; (H) granule-bearing sandstone
640 beds with centimetre-scale claystone partings (*lithofacies 4*) and one 3-cm-thick bed (black arrows) of isolated
641 finer-grained sandsheet (*lithofacies 6*) is interbedded within the granule-bearing sandstone package; (I)
642 sandpatch heterolithic sandstones (*lithofacies 5*) show deformed isolated sandy ripples within a matrix of dark
643 silty clay with floating fine to coarse grains. Ripples are composed of a mixture of fine and coarse grains; (J)
644 sandpatch heterolithic sandstones interbedded with granule-bearing sandstone show a wavy and poorly
645 defined basal contact with underlying sandstones; (K) thick package of ripple-laminated sandstones
646 (*lithofacies 8*) with centimetre-scale basal erosion with wavy upper contacts. Beds are often amalgamated but
647 thin clay partings are locally preserved; (L) ripple-laminated sandstones (*lithofacies 8*) show ripples in the
648 upper part and claystone drapes; (M) interference ripples indicating wave reworking of current ripples,
649 preserved beneath a few centimetres of claystones (*lithofacies 11*); (N) dipping sandy foresets in heterolithic
650 claystones (*lithofacies 10*) (O) aeolian sandstones with steep foresets, highlighted by white arrows, and
651 intercalated with alluvial-fan deposits. Black arrows highlight the erosional contact of alluvial-fan deposits.

652
653 **Figure 6:** Detailed sedimentary section at Soley Cove. The main part of the section shows thick alluvial-fan
654 deposits that eventually fine upward (retrograding) and are intercalated with playa deposits.

655
656 **Figure 7:** Detailed sedimentary sections at Economy Point (4 sections across 1.5 km). The sedimentary
657 architecture shows channel-fill sandstones forming a large composite channel-belt complex intercalated with
658 levees and silty or shaly floodplain deposits. Palaeocurrents measured from 41 fluvial cross-bed strike gives a
659 mean palaeoflow to the NE.

660
661 **Figure 8:** Schematic facies architecture of the highly faulted cliffs between Red Head and Soley Cove section
662 (roughly 4 km). Proportion of aeolian (white) and alluvial-fan (pebbles) sediments is represented. Shaded
663 conglomeratic packages are given in order to represent schematic initial architecture of interbedded aeolian
664 and alluvial-fan deposits but vertical small-displacement faults prevent a realistic reconstruction of primary
665 sedimentary architecture.

666

667 **Figure 9:** Correlation across the Minas sub-basin showing facies variability from south to north. Onset of
668 occurrence of finer-grained facies (such as sand-patch-fabric sandstones) and disappearance of aeolian beds
669 are used as time markers.

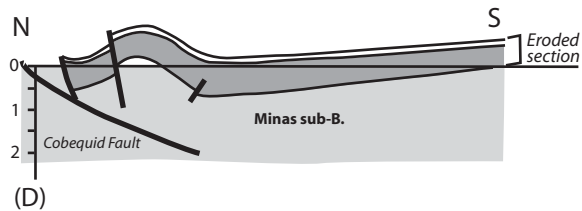
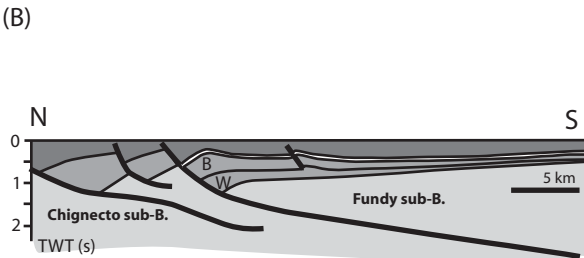
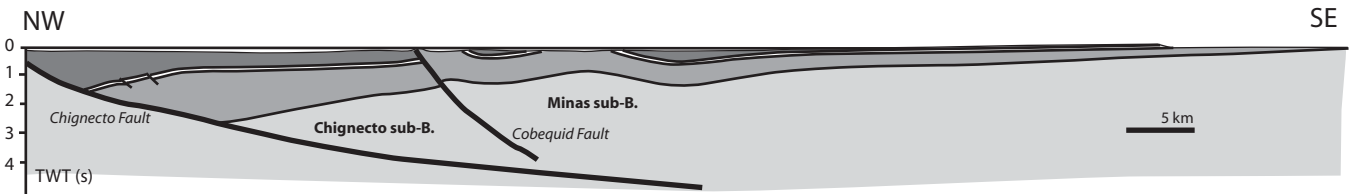
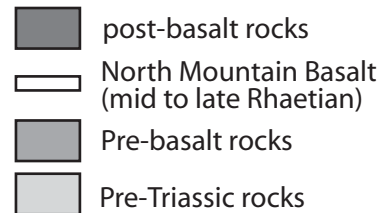
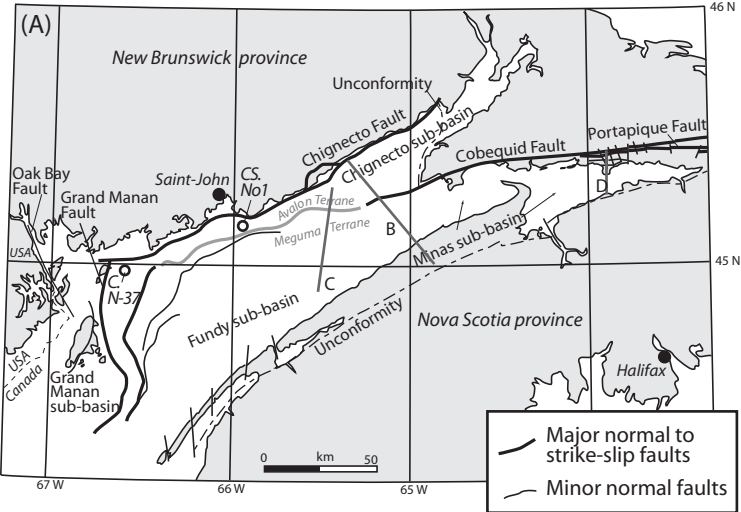
670

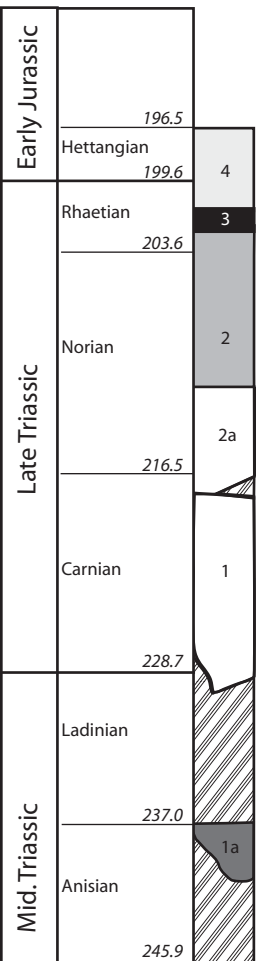
671 **Figure 10:** Sedimentary model for the period of horst development on the northern edge of the Minas sub-
672 basin, corresponding to the transition of upper Wolfville Formation and lowermost Blomidon Formation. The
673 depositional system was highly variable: close to the northern topography and along the fault scarp where
674 alluvial fans interfingered with aeolian dunes, abundant to the west. Aeolian sand was trapped in the small
675 drainage basins of the alluvial fans and was reworked into the matrix of fan deposits. Aeolian sand was
676 probably deposited on the downwind slope of the horst structure as wind mainly blew from the NW. Part of
677 the windblown sand was trapped in the catchment while most was deposited as aeolian dunes in the basin
678 along the fault scarp. In the southern part of the Minas sub-basin (Leleu & Hartley, 2010) aeolian dunes
679 interfingered with fluvial channels, terminal splays and shallow-lake deposits.

680

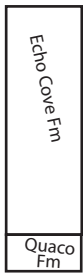
681 **Figure 11:** Triassic drainage evolution in the Fundy Basin; (A) Carnian (deposition of lower and middle
682 Wolfville Fm), the main depositional systems are transverse fluvial systems sourced from the hanging-wall
683 shoulder (south). The Cobequid High was not present. The longitudinal drainage is restricted to the northern
684 side of the basin in the Chignecto sub-basin; (B) early Norian (deposition of upper Wolfville Fm and
685 lowermost Blomidon Fm), the fluvial system of the hanging-wall decreased in size and terminated with splays
686 into a playa-type lake. An intrabasinal high emerged along the Cobequid Fault and small alluvial fans
687 developed. Aeolian dunes were relatively abundant in the basin and especially close to the fault scarp; (C)
688 upper Norian and lower Rhaetian (deposition of Blomidon Fm), the fluvial system decreased in size and splay
689 deposits dominated along the basin edge. Aeolian dunes and alluvial fans gradually disappeared along the
690 Cobequid High, suggesting that it was overlapped by the lacustrine facies. The playa facies eventually became
691 evaporitic in places.

692



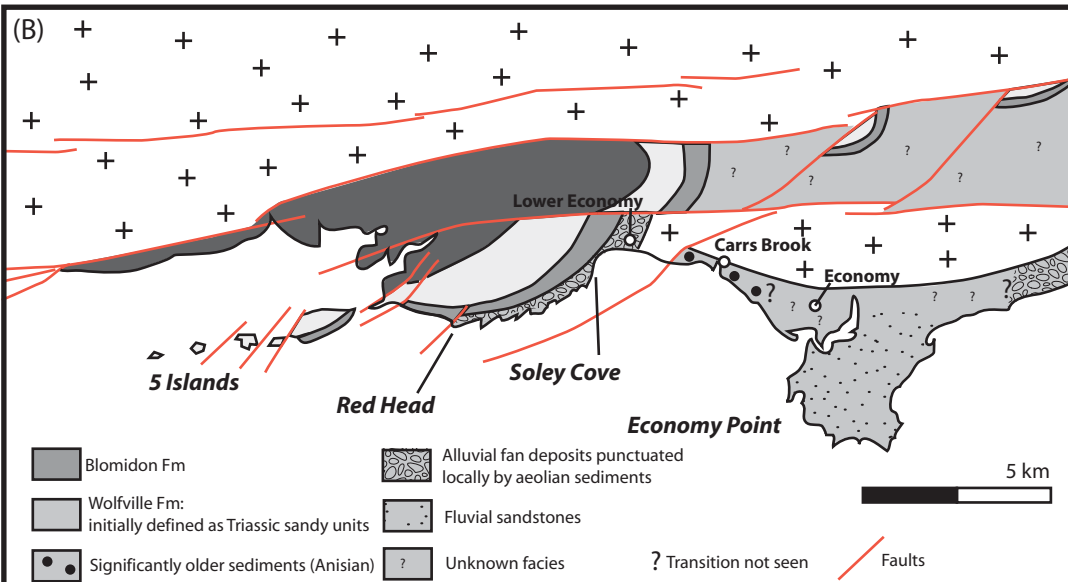
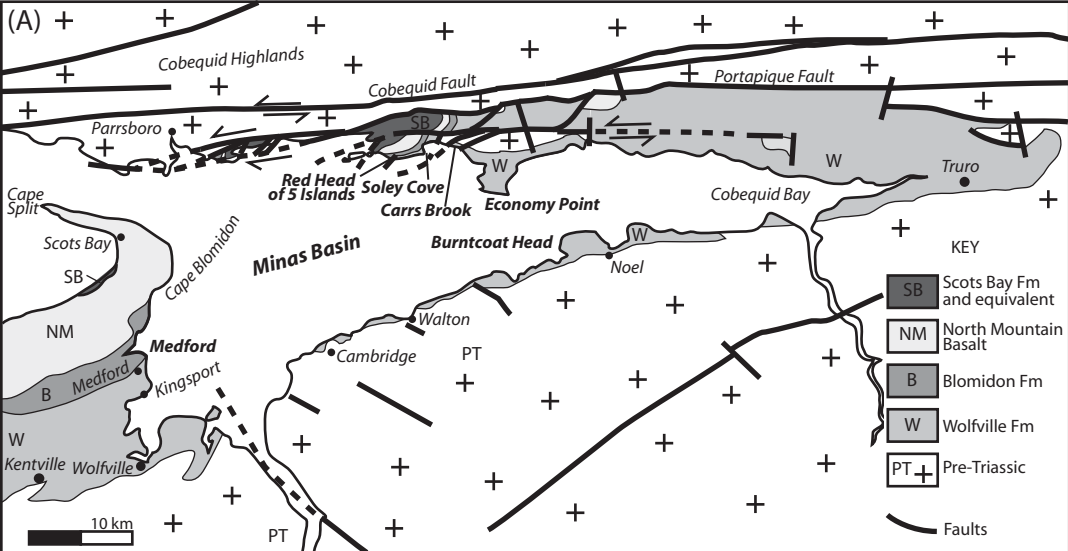


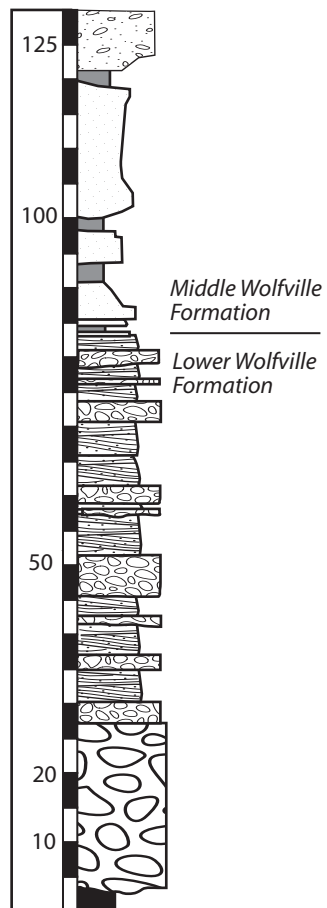
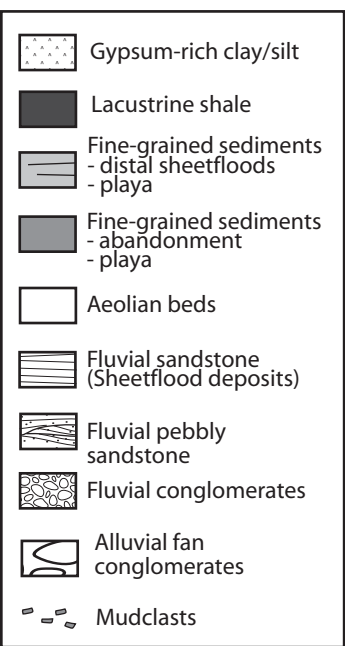
?



Chignecto sub-basin

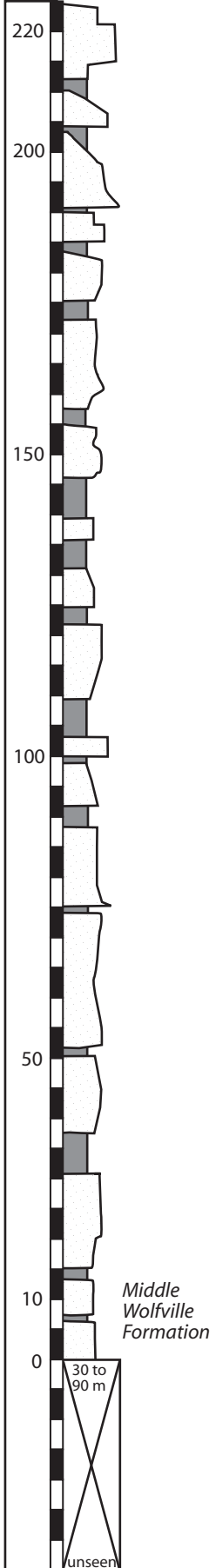
- 4: McCoy Brook Fm
- 3: North Mountain Basalt
- 2: Blomidon Fm
- 2a: Red Head Member of Blomidon Fm or Red Head Beds of Wolfville Fm
- 1: Wolfville Fm
- 1a: Lower Economy Beds, or Economy Beds, or Carrs Brook beds





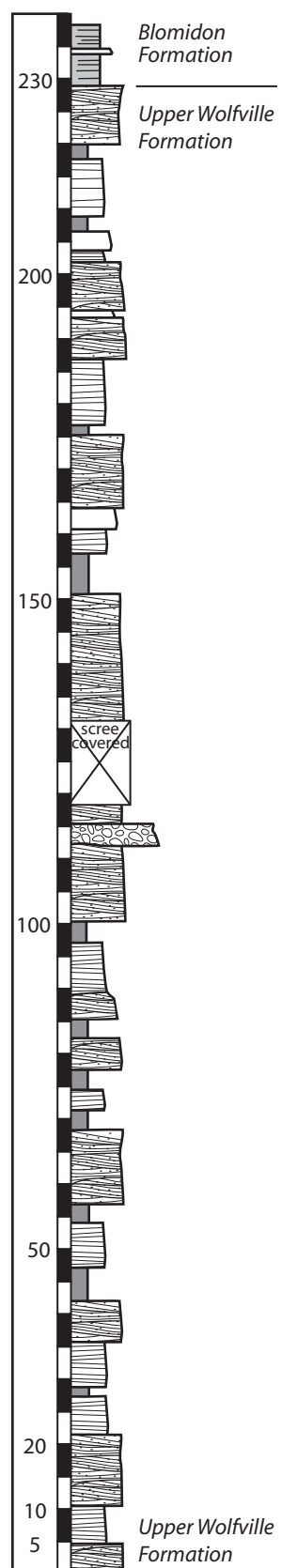
Southeastern shore Cambridge to Halfmoon Cove

(A)



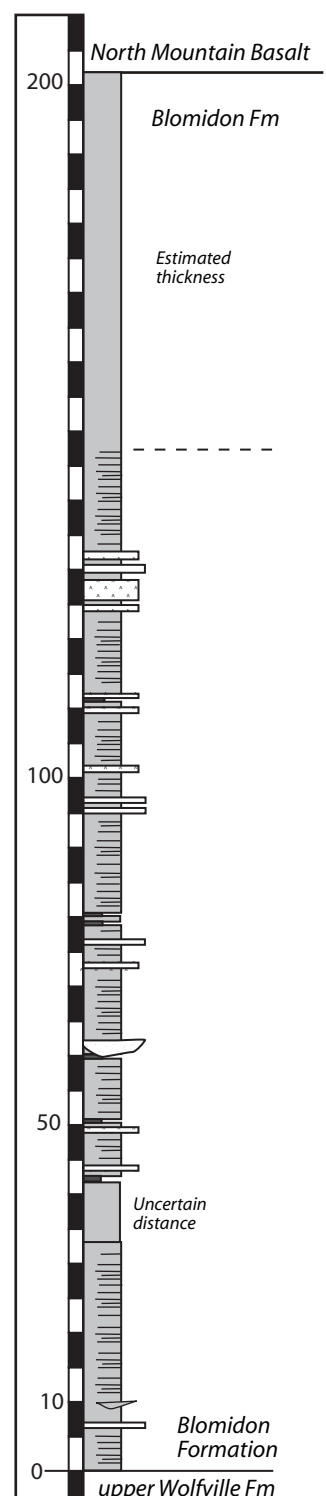
Burntcoat Head

(B)



Kingsport to Medford Beach

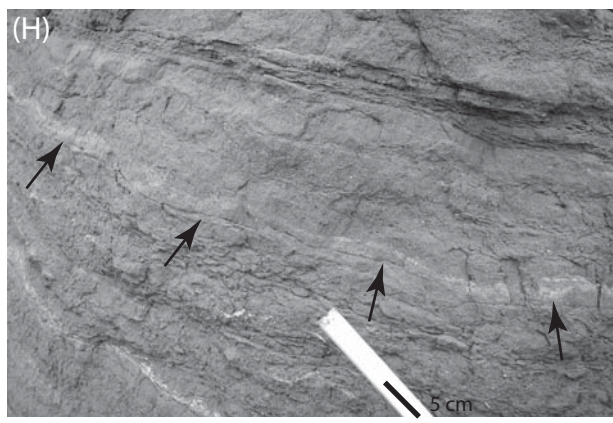
(C)

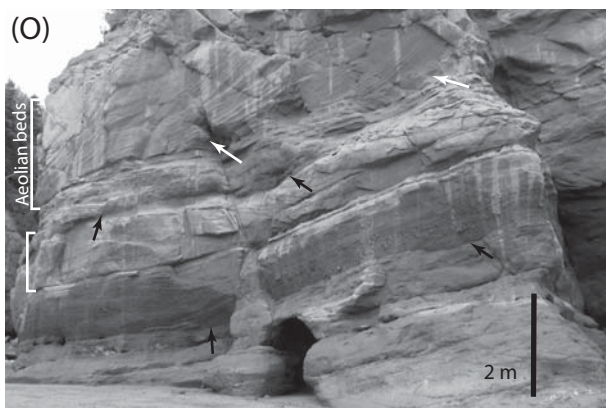
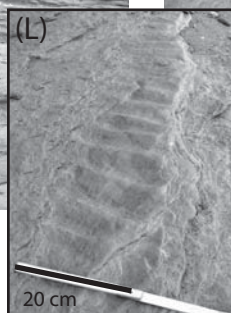


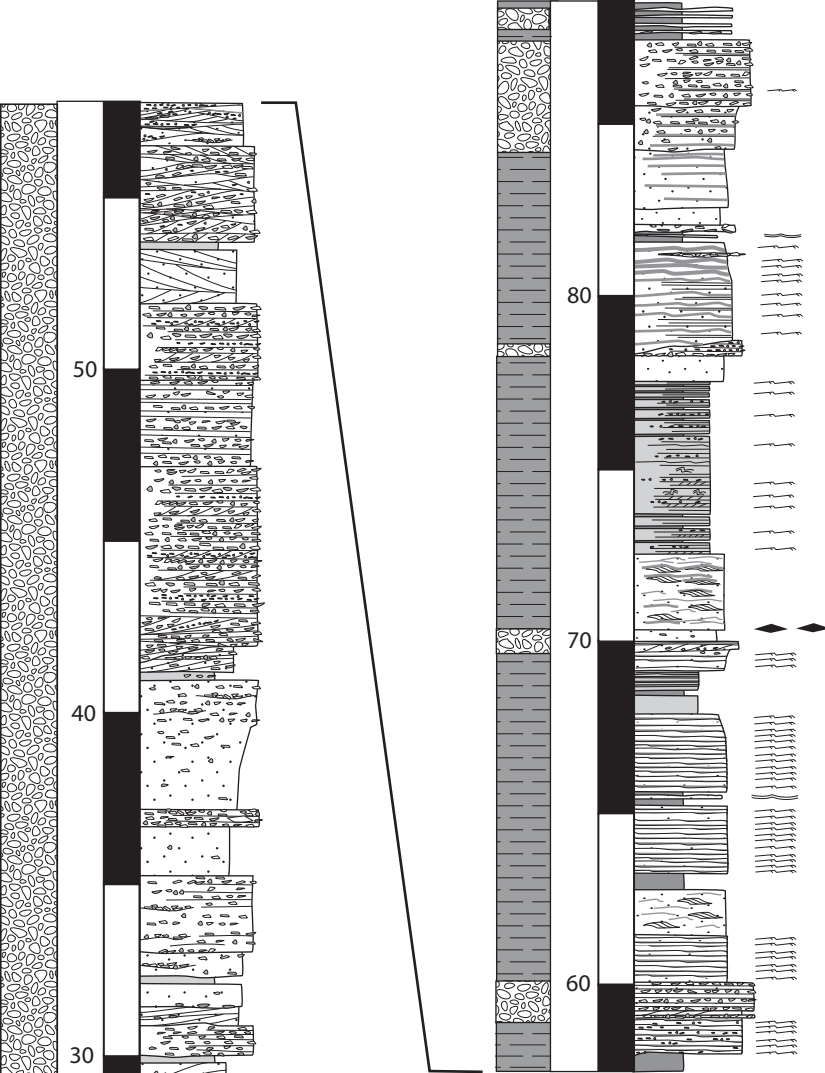
Medford Beach to Cape blomidon

(D)













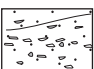
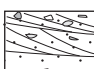
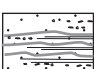
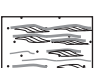
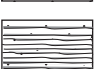
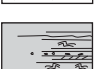

Facies associations

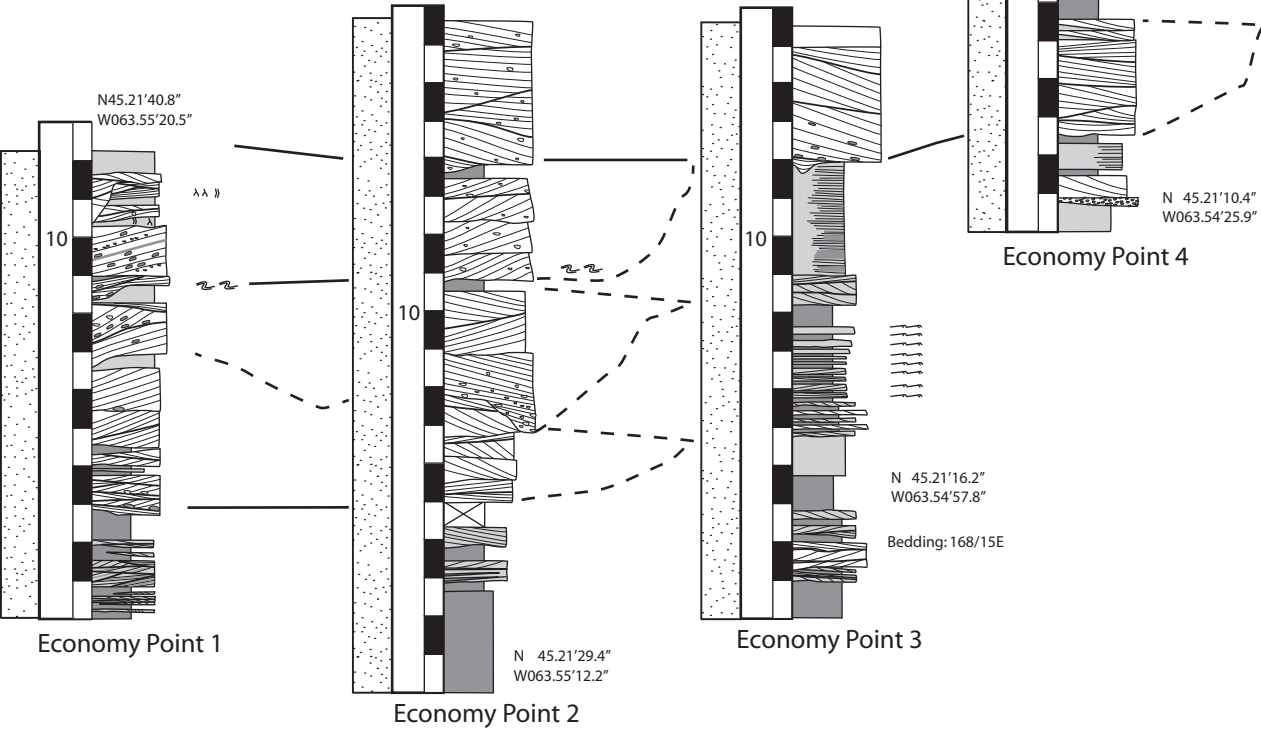
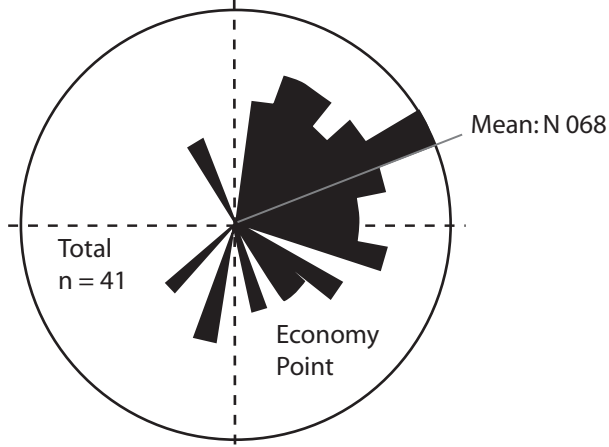
-  Alluvial fan FA
-  Fluvial FA
-  Playa margin FA

Sedimentary structures

-  Ventifact pebbles
-  Current ripples
-  Linguoid ripples

Lithofacies

-  Clast-supported breccia
-  Matrix-supported breccia
-  Massive or cross-bedded sandstone
Pebble-rich to pebble-poor
-  Granular sandstone
-  Sandpatch heterolithic sandstone
-  Ripple-laminated sandstones
-  Siltstone
-  Claystone



Sedimentary structures

- Current ripples
- Synsedimentary deformation
- Rootlets
- Bioturbation

Lithofacies

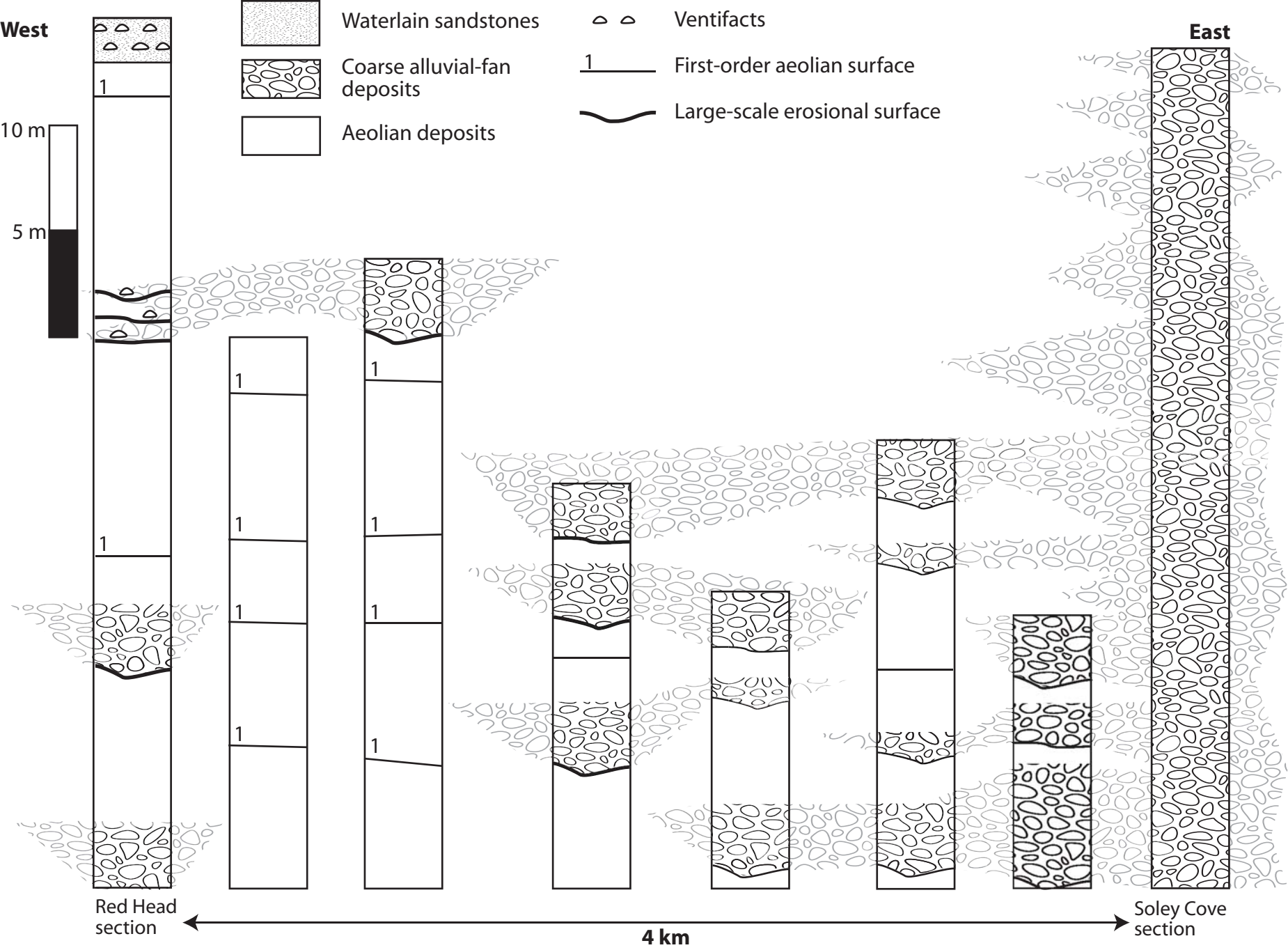
- Cross-bedded sandstone rare clasts and mudclasts
- Silty sandstone
- Siltstone
- Claystone

Facies associations:

- Fluvial FA

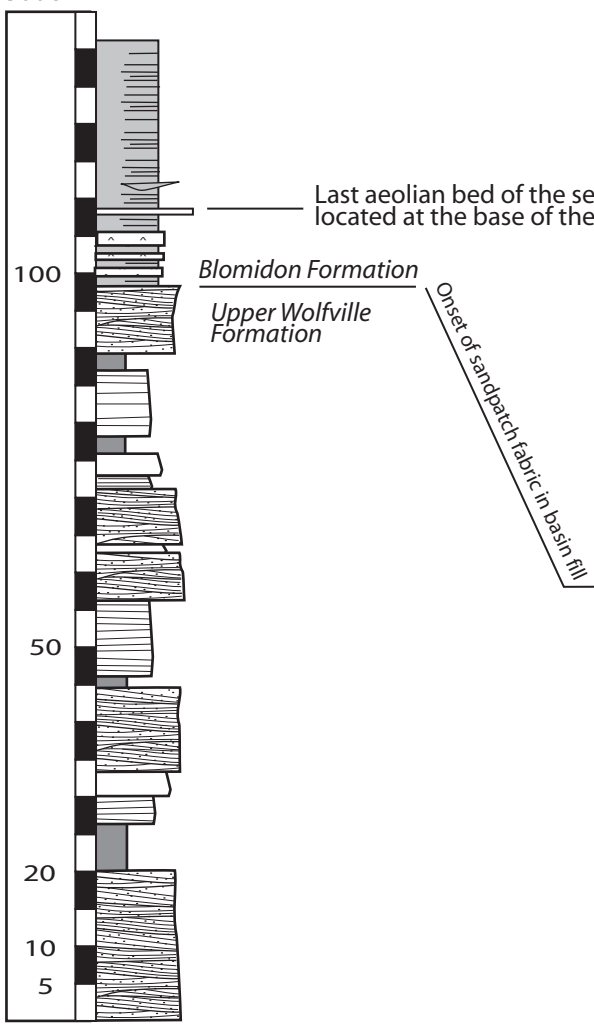
Correlations:

- from field observations
- interpreted channel fills, showing lateral floodplain deposits equivalent



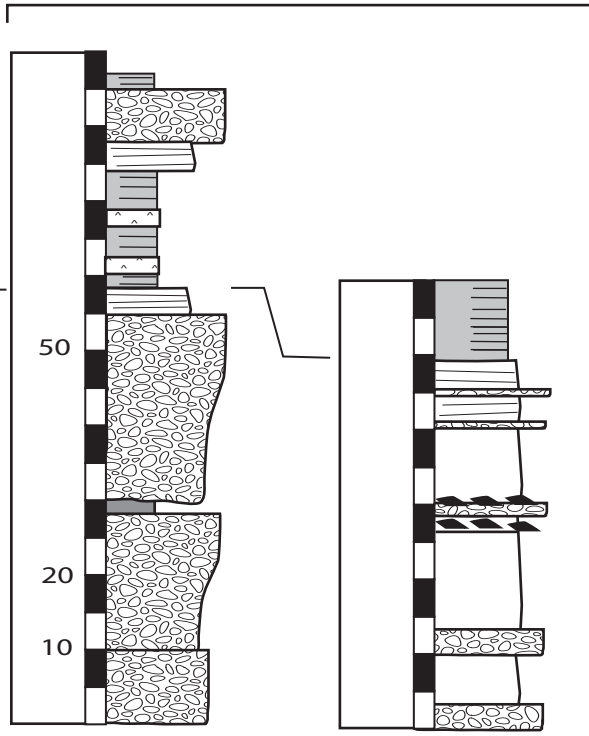


South



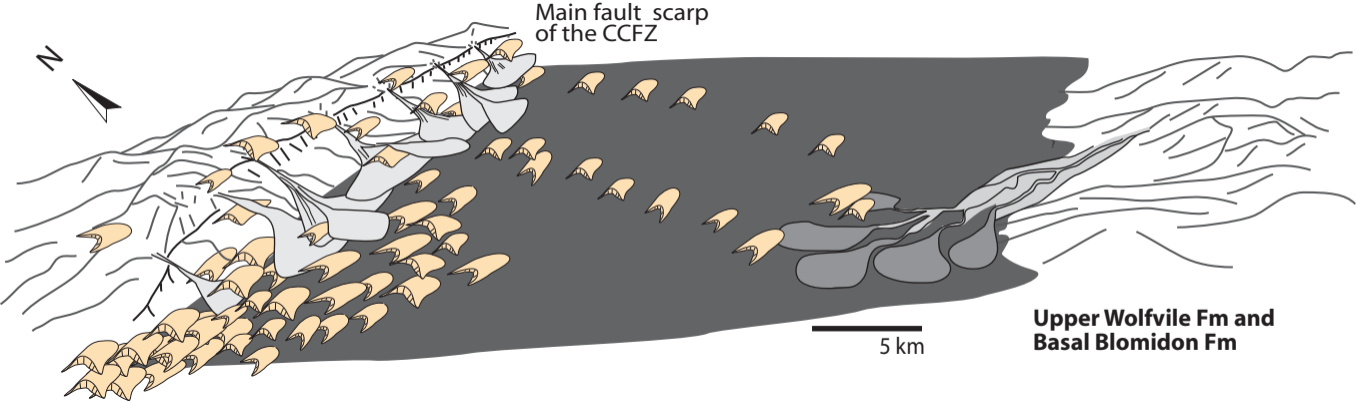
Medford Section, SW Minas sub-basin

North



Soley Cove Section, N Minas sub-basin

Red Head section, N Minas sub-basin

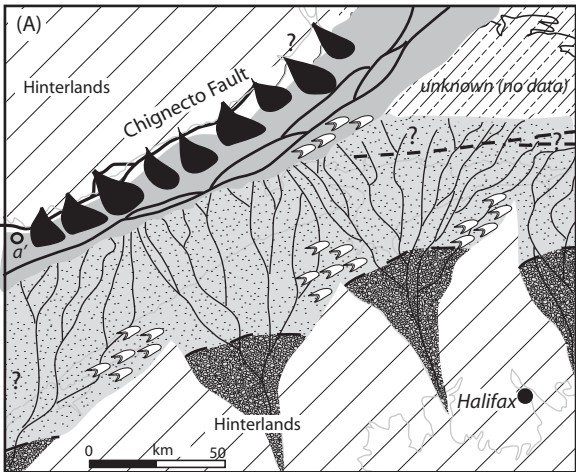


Main fault scarp
of the CCFZ

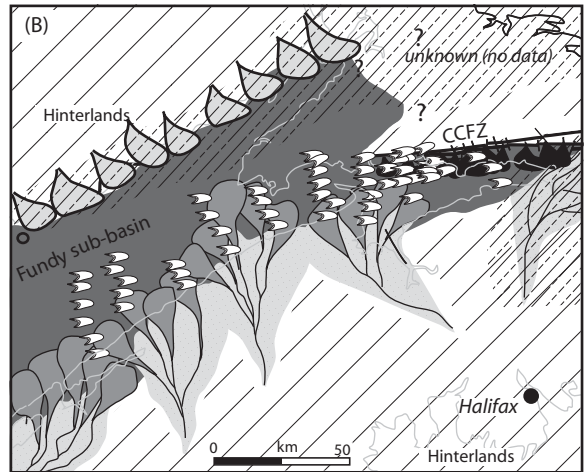


5 km

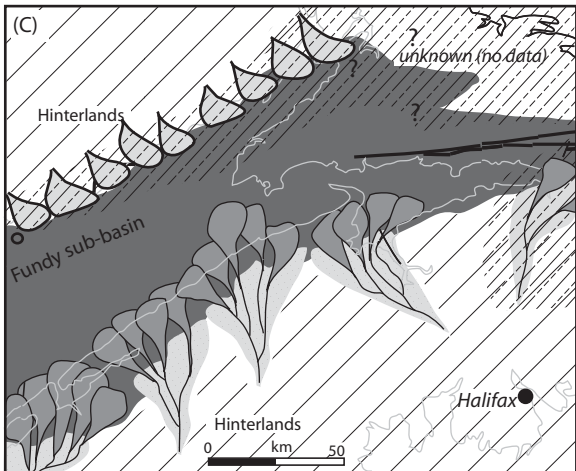
Upper Wolfvile Fm and
Basal Blomidon Fm



Wolfville Fm (Carnian)



uppermost Wolfville Fm / lowermost Blomidon Fm (early Norian)



Blomidon Fm (Norian to Rhaetian)

